# Development of a weighted sum estimate of the total radiated power from large helical device plasma



Review of Scientific Instruments

# Development of a weighted sum estimate of the total radiated power from large helical device plasma

Cite as: Rev. Sci. Instrum. **92**, 033518 (2021); https://doi.org/10.1063/5.0027302
Submitted: 28 August 2020 . Accepted: 07 February 2021 . Published Online: 05 March 2021

P. L. van de Giessen, G. Kawamura, S. Borling, K. Mukai, and B. J. Peterson

Review of Scientific Instruments ARTICLE scitation.org/journal/rsi

# Development of a weighted sum estimate of the total radiated power from large helical device plasma

Cite as: Rev. Sci. Instrum. 92, 033518 (2021); doi: 10.1063/5.0027302
Submitted: 28 August 2020 • Accepted: 7 February 2021 •
Published Online: 5 March 2021



P. L. van de Giessen,[1] G. Kawamura,[2,3] S. Borling,[4] K. Mukai,[2,3] and B. J. Peterson[2,3,a)]

## AFFILIATIONS

[1] Eindhoven University of Technology, Department of Applied Physics, 5612 AZ Eindhoven, The Netherlands
[2] National Institute for Fusion Science, Department of Fusion Science, Toki, Gifu 509-6292, Japan
[3] SOKENDAI (The Graduate University for Advanced Studies), Department of Fusion Science, Toki, Gifu 509-6292, Japan
[4] Whitman College, Department of Physics, Walla Walla, Washington 99362, USA

[a)] **Author to whom correspondence should be addressed:** peterson@lhd.nifs.ac.jp

## ABSTRACT

Diagnosing the amount of radiated power is an important research goal for fusion devices. This research aims at better understanding and diagnosing the radiated power from the Large Helical Device (LHD). The current radiated power estimate in the LHD is based on one wide-angle resistive bolometer. Because the estimate stems from one bolometer location toroidally and has a wide-angle poloidal view, this estimate does not take into account toroidal and poloidal radiation asymmetries that are observed in the LHD in discharges with gas puffing. This research develops a method based on the EMC3-Eirene model to calculate the set of coefficients for a weighted-sum method of estimating the radiated power. This study calculates these coefficients by using a least-squares method to solve for a coefficient set, using a variety of simulated cases generated by the EMC3-Eirene model, combined with corresponding geometric radiated power density considerations. If this set of coefficients is multiplied by the detector signal of each bolometer and summed up, this gives a total radiated power estimate. This new estimate takes into account toroidal and poloidal asymmetries by using the bolometer channels viewing different toroidal and poloidal locations, thereby reducing the estimation error and providing information about toroidal asymmetries.



## I. INTRODUCTION

Measuring the power radiated from the plasma inside fusion devices is an important diagnostic issue. Limiting the heat and particle flux reaching the divertor to prevent damage is one of the keys to developing feasible fusion energy power plants. One way to limit these fluxes is by seeding heavier impurity gases in the plasma edge regions to radiate power so that they do not reach the divertor. The ultimate goal is to reach plasma detachment, where the particle and heat fluxes to the divertor are limited, but the plasma core temperature is maintained. Diagnosing and understanding the behavior of the total radiated power is, therefore, necessary to improve plasma performance.

The Large Helical Device (LHD) heliotron is one of the larger helical devices currently in operation. The LHD focuses on investigating nuclear fusion phenomena in a twisted magnetic field configuration.

The current radiated power ($P_{rad}$) estimate in the LHD is based on multiplying an experimentally determined coefficient by the output of one wide-angle resistive bolometer.[1] When measuring from one toroidal location, this measurement has no poloidal or toroidal resolution. There is evidence that there *are* toroidal and poloidal radiation asymmetries in LHD discharges, especially after impurity gas seeding.[2,3] These radiation asymmetries can cause errors in the $P_{rad}$ prediction because they are distributed toroidally and poloidally over the plasma. Toroidal asymmetries occur in regions of the plasma that are not in the line of sight of the bolometer used for the measurement; using only one bolometer channel leads to a prediction error that is linearly related to the amplitude of the asymmetries. The toroidal radiation asymmetries are observed after

impurity gas seeding, and the discovered effects are dependent on the seeded impurity gas.[2,4] Identifying which type of gas minimizes the asymmetric effect could aid in improving plasma performance during gas seeding.

There are 44 working resistive bolometer channels available, spread out over three toroidal locations, as shown in Fig. 1. By including the signals from these channels in the estimate of the total radiated power, the toroidal and poloidal samplings can be improved because there is more information available from different locations in the plasma. Theoretically, using three toroidal bolometer locations instead of one should decrease the prediction error for the total radiated power due to toroidal asymmetry by around two-thirds on average, depending on the spatial distribution of the asymmetry.

This research aims at improving the estimate of the total radiated power by developing a weighted sum estimation with a coefficient set. Multiplying this coefficient set by the output of the bolometer channels and summing them should then give the total radiated power as accurately as possible. Calculating a coefficient set that follows these criteria can be done by using a least-squares solver for a large number of discharges with a known total radiated power and corresponding detector powers. Since this is not possible experimentally, EMC3-Eirene model data for the edge radiation are used combined with different artificial core radiation profiles. This combination gives multiple cases with an absolutely known total radiated power and corresponding detector outputs for a variety of discharge scenarios. With enough representative cases, the solver then gives a coefficient set, with which a total radiated power estimate can be made using all resistive bolometers. This method is similar to the method deployed in Ref. 5, which used regression analysis to find a coefficient set for a weighted sum. However, here the regression analysis is performed on simulated data and applied to multiple bolometers with a focus on toroidal asymmetries. Other work calculates coefficients for a weighted sum based on geometric considerations.[6,7]

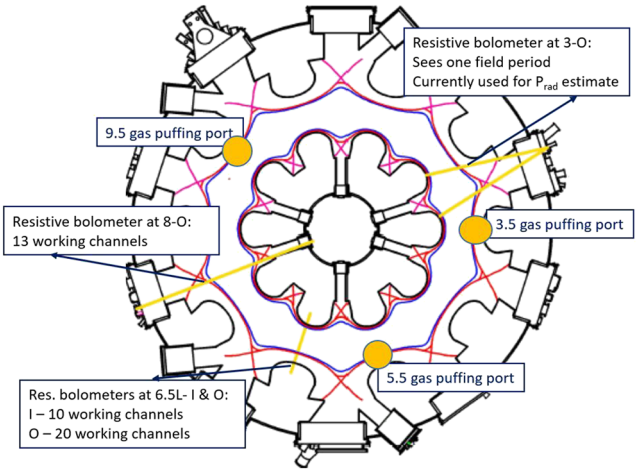


**FIG. 1**. LHD top view with the locations of the different bolometers given by their yellow lines of sight and gas seeding ports as given by their yellow circles and label. The LHD is divided into ten field periods with roughly the same characteristics.

The developed method of making a total radiated power estimate can additionally be applied to the separate bolometer array locations to study toroidal radiation asymmetry in the LHD. By analyzing the total radiated power estimates at different toroidal locations from different shots with different gas seeding characteristics and normalizing each signal to its value before the gas seeding, the relative change in radiation at each bolometer location gives a quantitative measure of the toroidal asymmetry. For N2, this is done in Ref. 8. This can be visualized for each different impurity gas. The differences in the normalized radiated power estimates after the gas seeding are a measure of toroidal radiation asymmetries.

In order to reach the aims of developing a radiated power estimate and analyzing toroidal radiation asymmetries in the LHD, this study's structure is as follows. First, it introduces the measurement setup, current radiated power measurement, and the EMC3-Eirene model in Sec. II. Then, in Sec. III, the process of creating the new coefficient set is specified, and expectations for the improvement of the estimate are given. In Sec. IV, the new estimate will be analyzed and compared to the old estimate. The conclusions of this study are highlighted in Sec. VI.

## II. BACKGROUND

This section describes the working principle and calibration of the resistive bolometer. Second, it gives an overview of the measurement setup that is used. Then, it details the current radiated power estimate, gives an account of the existing research concerning toroidal and poloidal asymmetries, and describes the EMC3-Eirene model.

### A. Resistive bolometers

A resistive bolometer is a diagnostic that measures the power coming from a radiation source. The bolometer integrates all the wavelengths that reach the bolometer, with the upper x-ray energy limit determined by the thickness of the bolometer foil. It is usually placed in a pinhole camera such that it has a line of sight to the radiation source, in this case, the LHD plasma. The wavelength integrated radiation from the plasma then heats the metal resistor in the detector. The increase in temperature changes the resistive properties of the metal, which is thermally connected to the radiation absorbing foil by an electrically insulating layer. The change in the resistance is subsequently measured and creates a voltage. This system has been calibrated using a laser with fixed $P_{\mathrm{rad}}$, to determine the sensitivity $K$ and the thermal time $\tau$ from the following equation:

$$P_{\mathrm{rad}} = \frac{1}{K}\left(V_b + \tau \frac{dV_b}{dt}\right). \tag{1}$$

### B. Measurement setup

The LHD is divided toroidally into ten field periods, each with one turn of the helical winding. At the integer numbered ports, the plasma has a horizontal elongation, and at the half-integer numbered "5" ports, the plasma has a vertical elongation. The inboard side ports are noted by "I," the outboard side ports by "O," and the upper and lower ports by "U" and "L," respectively. The locations

of the bolometer arrays and gas seeding ports are shown in Fig. 1. There are three different gas seeding locations: at 3.5-L, 5.5-L, and 9.5-L. There are four different locations with bolometers: one wide-angle bolometer at 3-O, two arrays at 6.5-L (one on the inboard side "i" and one on the outboard side "o"), and one array at 8-O. The lines of sight of the 8-O and 6.5-L bolometer arrays are, respectively, shown in Figs. 2 and 3. Each of the bolometers' channels has a different part of the plasma in their line of sight. Their output depends on the radiated power in that part of the plasma. The 3-O bolometer is uncollimated and has a broader view poloidally and toroidally.

Recently, there has been a change in the measurement setup. The 6.5-L-i bolometer array has been moved from outside the vacuum chamber to the inside. This has resulted in a loss of shielding from electron capture (EC) radiation, so during electron cyclotron heated (ECH) operation, this bolometer picks up ECH radiation and shows spikes.

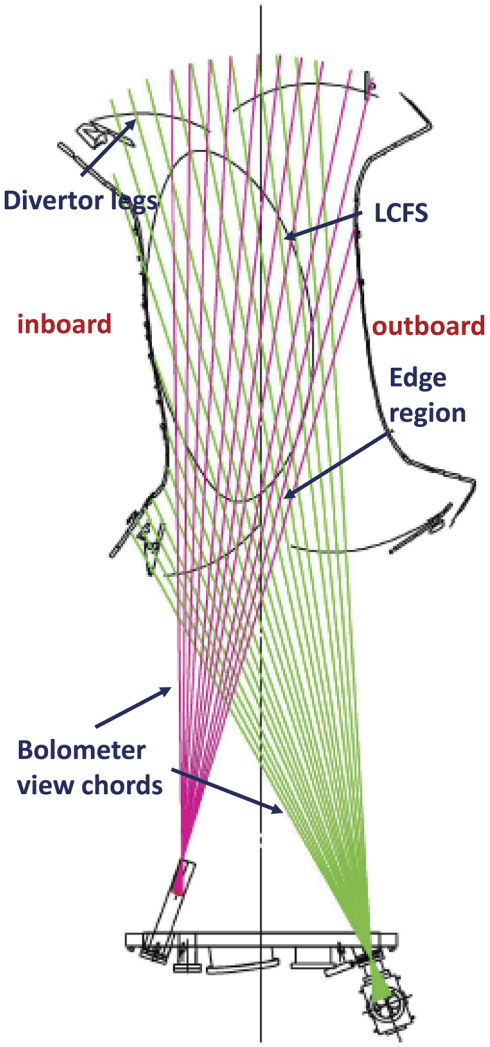


**FIG. 2**. Poloidal cross section of the 6.5L bolometers. Red lines indicate the outboard bolometer channels and green lines the inboard bolometer channels.

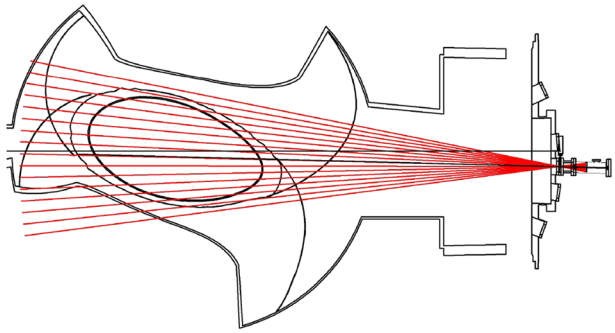

**FIG. 3**. Poloidal cross section of the 8-O bolometer.

### C. The current radiated power estimate

At the LHD, the current radiated power estimate is based on the power output of the 3-O bolometer. This bolometer has a wide viewing angle, viewing nearly the entire poloidal cross section and approximately one field period (36°) toroidally. The power output of the 3-O bolometer $P_{3-O}$ (in $\mu W$) is then multiplied by a coefficient $k\left[\frac{kW}{\mu W}\right]$ that relates the power at the detector with the actual radiated power. This gives an estimate of the total radiated power. This relative power coefficient was established experimentally as follows:[1]

1. The 8-O multi-channel resistive bolometer was used in a shot with standard operating parameters to perform tomographic inversion to find the radial profile of the radiated power density ($S_j$) profile, where $j$ is the index of the radial regions.
2. The radiated power density is multiplied by the volume $V_j$ corresponding to each radial region and summing this as $P_{\mathrm{rad}} = \sum_j S_j \cdot V_j$.
3. The coefficient is then found by dividing the total radiated power found in this procedure by the detector power of the 3-O bolometer at that same time. The coefficient is calculated by $k = \frac{P_{\mathrm{rad}}}{P_{3\text{-}O}}$.
4. The estimate of the total radiated power of all shots is now given by multiplying the detector power of the 3-O bolometer by this coefficient $P_{\mathrm{rad}} = k \cdot P_{3-O}$.

### D. Toroidal and poloidal asymmetry

Due to the helical winding, the LHD is not a toroidally symmetric device. Helical periodicity is most often assumed and means that every separate field period is identical. Toroidal radiation asymmetry is defined as the difference in radiation between the field periods. In addition, especially in the ergodic edge region outside the last closed flux surface (LCFS), the radiation is poloidally asymmetric, with radiation localized near the X-points of the helical divertor. In the regions of the plasma inside the last closed flux surface where the temperature is high, transport and, hence, equilibration are fast,

and the assumption of toroidal symmetry is natural. However, especially in the ergodic edge region, toroidal (radiation) asymmetry is a phenomenon that is observed from different diagnostics[2] and models.[4] Therefore, it is necessary to sample these different regions of the plasma to estimate the total radiated power accurately. The toroidal asymmetries are experimentally observed to be localized in the region next to the gas seeding port in the direction of a negative magnetic field. A recent study of nitrogen seeding with the developed method shows this behavior.[8]

### E. EMC3-EIRENE

EMC3-EIRENE is a 3D edge and divertor-leg transport model that incorporates fluid transport equations in the Edge Monte Carlo 3D (EMC3) code and kinetic transport equations with atomic molecular processes in the EIRENE code.[4,9] The model outputs the radiated power density distribution over its grid in the edge and divertor-leg regions for one helical field period in equilibrium. It does this for different input parameters: the densities of impurities, the magnetic field configuration, different heating methods, and more.[10] The precise equations that are taken into account have been documented.[11] There is qualitative agreement with the LHD plasma, as seen in comparing the EMC3-Eirene model with experiment[4] and in comparison of synthetic images with imaging bolometer images.[12]

## III. METHODOLOGY

This section describes how the set of coefficients is calculated. First, it details how a coefficient set for a weighted sum could be determined. Then, it explains how the cases to calculate the coefficient set were built up. Finally, the generated coefficients are tested on synthetic data.

### A. Making a coefficient set

The goal of this research is to make a set of coefficients that, when multiplied with the powers of their respective detectors and summed up, yields an estimate of the total radiated power $P_{\mathrm{rad}}$. So, a coefficient set $k_j$, multiplied by the detector output power $P_j$ at every detector channel and summed, should yield the total radiated power. For the run-time and data processing of the radiated power measurement, this should be one set of coefficients,

$$\sum_{j}^{channels} k_j P_j = P_{\mathrm{rad}}. \tag{2}$$

The same can then be applied to each of the bolometer arrays, at 6.5-L, 8-O, and the single wide-angle bolometer at the 3-O port. These coefficient sets for each bolometer port then allow the calculation of a local estimate of the total radiated power that can be used to study toroidal asymmetries. This could, for instance, be done by looking at the relative change in the estimates for different gas seeding scenarios.

The method that was previously used is the same but with only one detector channel and one experimentally determined coefficient: $P_{\mathrm{rad}} = k_{3-\mathrm{O}} \cdot P_{3-\mathrm{O}}$. Using more detectors, and thus having more coefficients, is beneficial because it increases the toroidal and poloidal resolution. The extended set of coefficients $k_j$ cannot be determined experimentally without "knowing" the actual radiated power, which was the problem to begin with.

Calculating the coefficients can be done for single bolometers by weighting the coefficients according to geometric considerations, as was done in Refs. 6 and 7. Here, more bolometer channels are used, and the actual radiated power is still not known.

Ideally, one would like to know $P_{\mathrm{rad}}$ and $P_j$ for a representative set of cases that represent as many different discharge scenarios in the LHD as possible. The system of equations with known $P_{\mathrm{rad}}$ and $P_j$ can then be fitted for the coefficients using a least-squares solver. The EMC3-Eirene model is deployed to generate a representative set of cases in order to solve for the coefficient set $k_j$. This coefficient set will still have an error, but the better poloidal and toroidal resolution that comes from increasing the number of detectors should give a better estimate than before.

### B. Generating the cases

Generating cases to train the coefficients is done by combining the EMC3-Eirene edge and divertor-leg radiation model with artificial core radiation densities and profiles. This is done for the case where the magnetic axis is at $R = 3.6$ m. Using this model approach has the advantage that the radiated power $P_{\mathrm{rad}}$ is known absolutely from the model, and the corresponding detector powers $P_j$ can be found from geometric considerations of the line of sight of each detector. Finding the detector powers for each case was done by using a synthetic analysis tool that has been successfully implemented in previous works.[4,10,13] In addition to using the EMC3-Eirene output, artificial toroidal asymmetries, core radiation, detector noise, and impurity radiation variations are added to the model. The following sections detail the buildup of the set of cases that is used to calculate the coefficients.

#### 1. EMC3-eirene cases

The EMC3-Eirene model is used to generate a set of cases for different and variable operating parameters. For each of these cases, it calculates the radiated power in the edge and divertor leg. The cases can be made for different densities, for instance, $[1, 2, 4, 8, 16, 32] \cdot 10^{18}$ m$^{-3}$ at the last closed flux surface (LCFS), and different powers crossing the LCFS, for instance, [1, 2, 4, 8, 16] MW. These sets of cases are also generated for different plasma compositions. For example, (1) no impurities (only deuterium) without core radiation, (2) deuterium with a carbon impurity and a flat core radiation profile, (3) and deuterium with a carbon impurity and a hollow core radiation profile. Different combinations of $P_{\mathrm{LCFS}}$ and $n_{\mathrm{LCFS}}$ are chosen, where for each $P_{\mathrm{LCFS}}$, a density was chosen such that the temperature in the core would remain above 50 eV. These are chosen to reflect different LHD operating scenarios. This makes for a total of 51 cases.

#### 2. Adding core radiation

Now, there are 51 cases with EMC3-Eirene calculated edge radiation. These are supplemented by artificial core radiation to get a full emissivity profile. The core radiation profiles are chosen to reflect the core radiation profiles as present in different LHD discharges in agreement with a previous study.[14] The core of the LHD

is divided into four radial regions, from radially outward to radially inward based on vacuum magnetic flux surfaces. The different imposed core radiation power densities and power density profiles in cases [2] and [3] are varied so as to include as many possibilities as possible in the calculation of the coefficients. In the flat power density profile case, the radiated power density itself is varied but is equal in each section of the core. In the hollow core radiation profile cases, the radiated power density in every one of the core regions is varied. For every EMC3-Eirene case, 30 different core radiation power densities and power density profiles are used. Now, there are $51 \times 30 = 1530$ cases.

#### 3. Adding toroidal asymmetry

In order to better take into account toroidal asymmetry, an artificial sinusoidal asymmetry is added to the data. This toroidal asymmetry mimics one possible form of a toroidal asymmetry. The purpose is mostly to optimally distribute the weighting of the coefficients over the channels at the different toroidal locations. It is added to the model with a starting point $\phi$ that varies every $5^\circ$ to the cases in the following way: $P_{\mathrm{det_a}} = (1 + A \sin(\phi + f \cdot \omega)) \cdot P_{\mathrm{det}}$, where A is the amplitude of the toroidal asymmetry, $\omega$ is the location of each bolometer toroidally, $P_{\mathrm{det}}$ is the original synthetic power reaching the detector, and $P_{\mathrm{det_a}}$ is the new power reaching the detector after adding asymmetry toroidally. This gives 72 times more cases for the calculation of the coefficients, which now consists of $51 \times 30 \times 72 = 110\,160$ cases.

#### 4. Adding noise

Random noise is added to the model detector signals for multiple reasons. First of all, bolometers have noise, so it is a representation of a physical phenomenon. By adding noise, the weighting of the coefficients should be more evenly spread over the bolometer channels and, thus, decrease the possibility of noise being picked up in the signal. Second, adding noise to the model prevents the existence of unrealistic singular solutions to the coefficient set, with some very high coefficients and some negative, indicating that somehow one slice of plasma would account for three times the total radiated power and another slice for "negative radiation," which would only have a mathematical meaning. Finally, not all possible scenarios are taken into account in the cases, and adding noise would add to the robustness of the set by diminishing the case-specificity of the coefficients.

The noise is added to each detector separately; a new random number is generated for every detector for every case in the following manner: $P_{\mathrm{det_n}} = (1 + B \cdot R_N) \cdot P_{\mathrm{det}}$. With B the chosen amplitude of the detector noise, $R_N$ is a random number chosen from a normal distribution, $P_{\mathrm{det}}$ is the original synthetic power reaching the detector, and $P_{\mathrm{det_n}}$ is the new power reaching the detector after adding noise.

#### 5. Analyzing the set of cases

Using this set of cases, which now consists of 110, 160 cases, a coefficient set can be produced with the least-squares solver. The variables in the production of this coefficient set are now the amplitude of the: toroidal asymmetry, detector noise, and the different hollow core profiles. These variables have a physical representation, but they can also be interpreted as computational aid to make the coefficient set more robust. The problem of making a coefficient set is in some sense a tomographic problem, identifying for each detector what part of the plasma is in its line of sight. More variation in the different regions should, therefore, increase the prediction accuracy. The artificial toroidal asymmetry distributes the radiated power prediction over the three available bolometer array locations. The detector noise amplitude distributes the radiated power prediction on each bolometer array location over the different available channels instead of giving one coefficient a very high value, which could be considered non-physical. Furthermore, the higher the amplitude of the artificial detector noise, the fewer the negative coefficients are found.

### C. Neglected channels

Apart from deleting malfunctioning detector channels, other channels were deleted. These channels either were located in the far edge and had more noise than the signal, had a negative signal, or predicted the amount of total radiated power on their own that was more than 30% of the total radiated power prediction at that bolometer. The existing channels indicate that there could be some mismatch between the EMC3-Eirene model and experiment in these regions since the lines of sight of these deleted channels were mostly pointed toward the outer core of the plasma, which is where some discrepancy might arise. After deleting these channels, coefficients were recalculated for the remaining detectors.

### D. Testing the coefficient set on synthetic data

The calculated set of coefficients is tested to analyze its behavior on the synthetic data. This is done by testing the coefficient set on the 110 160 cases for different toroidal asymmetry amplitudes (TAAs) and comparing this to the old estimate behavior. In addition, the separate total radiated power estimates of the 6.5-L and 8-O bolometers are shown. The average absolute prediction errors are shown in Table I. One observes that the single bolometer estimates are more affected by toroidal asymmetries and that the 8-O and 6.5-L bolometers, having more lines of sight, have a slightly lower error than the 3-O estimate.

**TABLE I**. The average absolute estimation error of the different estimate over the 110 160 synthetic cases, with different applied values for A, the Toroidal Asymmetry Amplitude (TAA) as described in Sec. III B 3. All cases have an applied detector noise of B = 0.1, as defined in Sec. III B 4. It is visible that the new total radiated power estimate is less affected by the artificial asymmetries than the single bolometer estimates.

| Avg. estimation error | 0 TAA (%) | 0.1 TAA (%) | 0.2 TAA (%) | 0.3 TAA (%) | 0.4 TAA (%) |
|---|---|---|---|---|---|
| New estimate | 7.5 | 7.8 | 8.7 | 9.9 | 11.3 |
| Old estimate | 14.9 | 15.7 | 18.1 | 22.2 | 27.1 |
| 3-O estimate | 13.9 | 15.0 | 17.7 | 21.6 | 25.9 |
| 6.5-L estimate | 9.4 | 11.7 | 15.3 | 19.1 | 23.1 |
| 8-O estimate | 8.1 | 10.0 | 13.8 | 17.9 | 22.5 |

## IV. RESULTS

In this section, the calculated set of coefficients is applied to experimental data of different shots. The results are structured in the following way: First, the new total radiated power estimate is compared to the current radiated power estimate for different shots. Then, toroidal asymmetries during different gas seeding and magnetic field scenarios are analyzed by normalizing to just before gas seeding and measuring the relative changes in radiation.

### A. Absolute total radiated power estimates

The old and new radiated power estimates are shown with different shots in Figs. 4 and 5. When there is no gas seeding, the estimates are in agreement. Overall, the new estimate seems to give a higher total radiated power estimate than the old estimate when there is gas seeding. This is visible after neon seeding in Fig. 5. In order to understand the differences between the old and new radiated power estimates, consider the supplemented total radiated power estimates from each of the separate toroidal locations, at ports 3-O, 8-0, and 6.5-L.

The new estimate acts as a form of "average" between the two extremes, which implies that the prediction error arising from the toroidal asymmetry caused by the gas seeding is decreased with the new estimate. This analysis gives insight into the behavior of the new total radiated power estimate compared to the old one. For shot 151 714 in Fig. 5, the estimate based on the 6.5-L bolometer arrays, which are close to the neon gas seeding port 5.5-L, shows a higher total radiated power estimate than $P_{new}$ after neon seeding than before, whereas before neon gas seeding, the estimate from 6.5-L aligns with $P_{new}$ almost indistinguishably. Figure 4 shows that the new estimates from ports 6.5-L and 8-O give values similar to the new total radiated power estimates when there is no toroidal radiation asymmetry. The separate bolometer estimates do, however, show a spread in their estimates. An estimation error is expected, especially in the separate bolometer estimates. These results imply that, indeed, the prediction error during toroidal asymmetries could be decreased by using more bolometer locations.

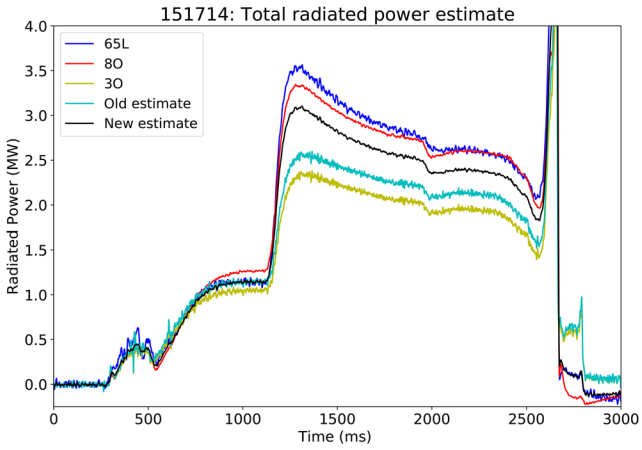


**FIG. 5**. Total radiated power estimates for shot 151 714 including separate port estimates. After neon seeding at 1000 ms from port 5.5-L, all the estimates increase. However, the estimates of the 6.5-L and 8-O bolometers increase a lot more than the old estimate and the estimate of the 3-O bolometer, indicating a toroidal asymmetry. This toroidal asymmetry appears to start in the gas seeding port 5.5-L and "move" in the direction opposite to the magnetic field, which has a negative direction in this case. The distance between the seeding port and the bolometers is 2.5 field periods, but the 8-O bolometer estimate increases by a factor of 2.7 and the 3-O bolometer by a factor of 2.3.

### B. Toroidal asymmetry from gas seeding

The new, the old, and the single bolometer radiated power estimates are shown for different shots with different impurity gas seeding. The estimates are normalized to just before the impurity seeding

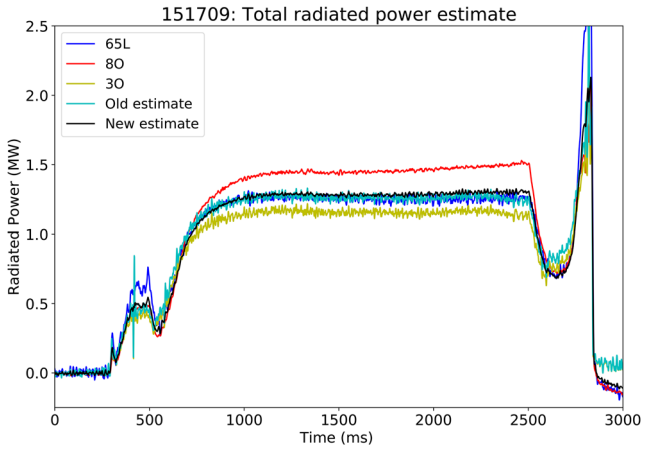


**FIG. 4**. Total radiated power estimates for shot 151 709, including separate port estimates. Apart from the 8-O estimate, they are mostly in agreement. An 8-O calibration error should be considered.

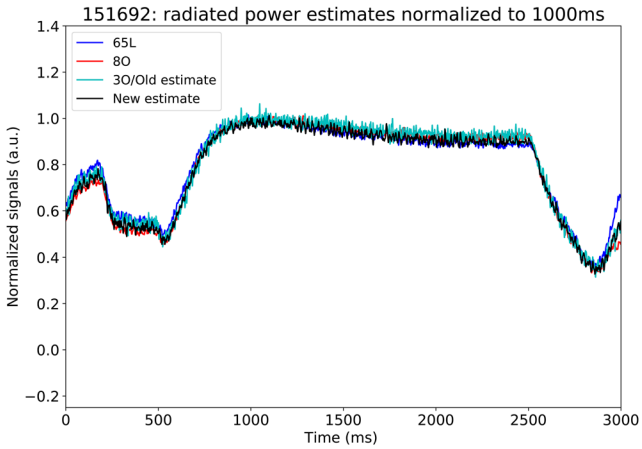


**FIG. 6**. All estimates for shot 151 692 without gas seeding; the signals are normalized to 1000 ms. As expected, without gas seeding, the estimates from the different bolometer locations show no relative change. There is ECRH pickup between 0 ms and 200 ms.

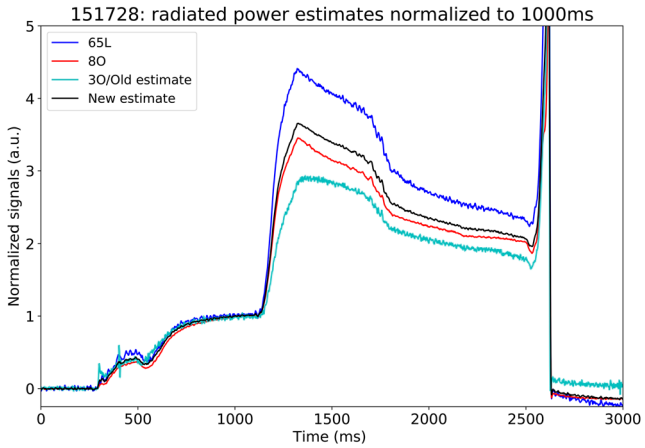


**FIG. 7**. All estimates for shot 135 506 with neon seeding from port 5.5-L at 1100 ms, with normalization at 1000 ms. This figure of normalizing the estimates shows that toroidal asymmetries can be analyzed by looking at the relative increase in radiation for each bolometer port.

to observe the relative changes in the estimates instead of the absolute changes, which are prone to absolute error. Most shots that are shown have gas seeding from port 5.5-L, as this port is in between the detectors, and thus, the toroidally asymmetric effects are more easily interpreted and analyzed.

### *1. Without gas seeding*

First, a shot without gas seeding is shown as a reference. As expected, Fig. 6 shows that when there is no impurity gas seeding, there is no radiation asymmetry; all estimates show the same relative behavior, except when the ECH is turned on, then the 6.5-L bolometer prediction shows the ECH pickup.

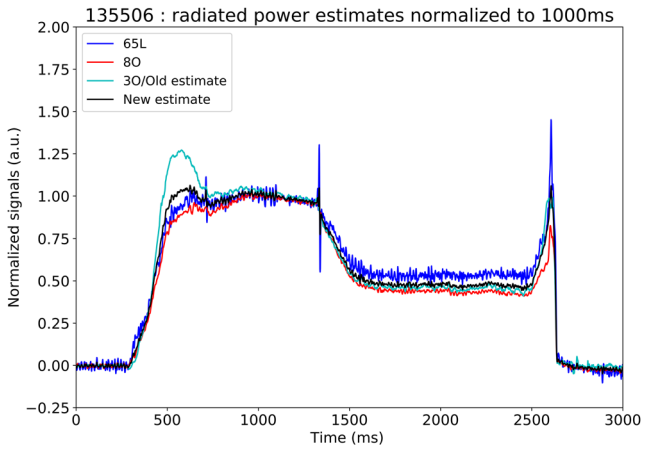


**FIG. 8**. All estimates for shot 135 506 with $D_2$ seeding from port 3.5-L at 400 ms, with normalization at 1000 ms. A small toroidal asymmetry is observed for the $D_2$ seeding phase. This asymmetry vanishes over time.

### *2. With gas seeding*

During gas seeding, normalizing the radiation estimates to before the gas seeding gives insight into toroidal asymmetries. In Fig. 7, a toroidal asymmetry is visible after neon seeding. During fueling, where $H_2$ or $D_2$ gas is seeded, there is sometimes also evidence of some radiation asymmetry. This does not occur in every fueling shot, but does appear to happen during $D_2$ seeding. One example is given in Fig. 8. Here, $D_2$ seeding from port 3.5-L leads to higher radiated power predictions at the 3-O port bolometer. Afterward, the signals converge, so the asymmetry seems to disappear when the deuterium particles distribute over the device.

## V. DISCUSSION

The results show that the new radiated power estimate behaves differently than the old measurement during gas seeding. This implies that it takes into account toroidal asymmetries. Furthermore, the new estimate predicts similar values to the old estimate when there is no gas seeding. The prediction error due to toroidal radiation asymmetries seems to have decreased, by the apparent "averaging" of the new radiated power prediction with respect to the different single bolometer estimates, which is also seen in modeling with the synthetic data.

The use of the weighted-sum method to estimate $P_{\mathrm{rad}}$ is valid if enough of the plasma is sampled in the lines of sights of the utilized bolometers. The validity of the coefficients is dependent on the EMC3-Eirene model that is employed to give the edge and density radiation profiles. Furthermore, the amount of cases and choices in profiles that is inputted in the calculation of EMC3-Eirene and the cases could affect the coefficient set slightly. In general, making one fixed coefficient set in the weighted-sum method that is accurate for all discharge scenarios is impossible. Different operating temperatures, densities, impurity types, and impurity densities can affect the radiated power estimate. For the purpose of this paper, a choice is made to generate a coefficient set that is most optimal on average due to the fact that it can then be implemented in LHD real-time data processing. The new radiated power measurement close to the old (experimental) measurement in scenarios without gas puffing is encouraging in this respect. However, some channels were deleted that predicted more than 30% of the radiated power of that bolometer. These channels might indicate a mismatch between EMC3-Eirene and experiment at least in some parts of the plasma. The new total radiated power measurement also takes into account toroidal asymmetries, as opposed to the current estimate, where its value should mostly be allocated, especially when it is used as a supplemental radiated power measurement in the LHD.

The method to analyze toroidal asymmetries yields information about toroidal asymmetries after gas seeding. Due to the normalization before gas seeding, the absolute calibration of the bolometers and the match between EMC3-Eirene and experiment are less consequential. The signals now show the relative changes in radiation in the plasma. The results show that there are toroidal radiation asymmetries after gas seeding. These results confirm and help quantify the amount of toroidal asymmetry present in the LHD after impurity gas seeding. The asymmetries appear to move in the opposite direction of the magnetic field from the gas seeding port, which is in line with earlier results.

The results indicating toroidal asymmetry are strengthened by the fact that when there is no gas seeding, there is no relative difference between the bolometer estimates.

Normalizing to before the impurity puffing can decrease the problem of absolute or calibration errors. However, normalization might bring another problem with it, if deuterium is puffed in the fueling phase before normalization, that influences the relative power measurements. Furthermore, the location from which different impurity gases radiate can differ. Since not all impurity gases were taken into account in the calculation of the coefficients, this could result in considerable relative differences between the bolometer signals, especially in the comparison of the bolometer signals from half-integer and integer locations.

Toroidal asymmetries are localized effects, and they can have large amplitudes. That the radiation does not fully equilibrate, that is, the radiation asymmetries do not seem to entirely vanish over time in the neon case is strange. One would expect this to eventually happen when the gas distributes over the torus. It could be that the time of the shots was short on this time scale or that part of the impurity remains in the cold edge and, therefore, does not distribute around the plasma. More research is necessary to find out exactly why these radiation patterns do not converge. This could, for instance, be done by seeding an impurity gas, maintaining the shot for a longer time and observing whether the asymmetry disappears.

## VI. CONCLUSION

A new method to estimate the radiated power coming from LHD plasma was developed. This method multiplies the powers at all available resistive bolometer channels and sums them up by a corresponding coefficient to give a $P_{rad}$ estimate. This method solves for a coefficient set using a least-squares solver with 110 160 synthetic cases. The new radiated power estimate takes into account toroidal asymmetries, as it uses three toroidal bolometer locations. In addition, it gives a higher radiated power estimate for most shots. So, although there might well be a prediction error, it is suggested that this new estimate could be used as an additional radiated power estimate for the LHD because it generates information about toroidal asymmetries after gas seeding. This method will also be used to generate new estimates for other standard magnetic configurations, $R = 3.75$ m and $R = 3.9$ m.

Using total radiated power estimates from separate bolometer arrays located at different toroidal locations, an analysis method for toroidal asymmetries was developed. This analysis gives insight into the toroidal radiated power distribution and changes therein. Toroidal asymmetries were observed for neon impurity seeding. The asymmetric effect might be countered by seeding from all three gas seeding ports at once.

Future work to extend on this research could be one of the following. Neural networks could be used to include the different plasma conditions in the calculation of the coefficient set, as done in Ref. 15. Highly radiative shots, where the input power should be the same as the output power, could be used to calibrate the coefficient-set method. The lines of sight of the video bolometer that is installed in the LHD could also be used to improve the results and verify and identify the radiation profiles. Furthermore, a method using singular value deposition, similar to Ref. 5, might be used to decrease the amount of detectors used and make the method more robust.

## ACKNOWLEDGMENTS

This work was done with the support of the National Institute for Fusion Science Research (Grant No. NIFS15ULHH026). This work was carried out within the framework of the EUROfusion Consortium and received funding through FuseNet from the Euratom research and training program (Grant Agreement No. 633053). The views and opinions expressed herein do not necessarily reflect those of the European Commission.

## DATA AVAILABILITY

The data that support the findings of this study are available from the LHD. Restrictions apply to the availability of these data, which were used under license for this study. Data are available from the authors upon reasonable request and with the permission of the LHD board.

## REFERENCES

[1]B. J. Peterson, A. Y. Kostrioukov, N. Ashikawa, Y. Liu, Y. Xu, M. Osakabe, K. Y. Watanabe, T. Shimozuma, and S. Sudo, "Bolometer diagnostics for one- and two-dimensional measurements of radiated power on the Large Helical Device," Plasma Phys. Controlled Fusion **45**, 1167–1182 (2003).

[2]B. J. Peterson, G. Kawamura, H. Tanaka, R. Sano, K. Mukai, S. Y. Dai, S. Masuzaki, T. Akiyama, M. Kobayashi, S. N. Pandya, M. Goto, G. Motojima, R. Sakamoto, N. Ohno, T. Morisaki, and J. Miyazawa, "Experimental observations and modelling of poloidal asymmetries in radiation profiles during $N_2$ seeding compared with Ne seeding in LHD," Technical Report, 2016.

[3]H. Tanaka, G. Kawamura, S. Masuzaki, M. Kobayashi, T. Akiyama, B. J. Peterson, K. Mukai, R. Sano, S. Y. Dai, R. Sakamoto, T. Morisaki, and N. Ohno, "Toroidally symmetric/asymmetric effect on the divertor flux due to neon/nitrogen seeding in LHD," Nucl. Mater. Energy **12**, 241–246 (2017).

[4]G. Kawamura, H. Tanaka, K. Mukai, B. Peterson, S. Y. Dai, S. Masuzaki, M. Kobayashi, Y. Suzuki, and Y. Feng, "Three-dimensional impurity transport modeling of neon-seeded and nitrogen-seeded LHD plasmas," Plasma Phys. Controlled Fusion **60**, 084005 (2018).

[5]M. Maraschek, J. Fuchs, K. Mast, V. Mertens, and H. Zohm, "Real-time determination of total radiated power by bolometric cameras with statistical methods," Rev. Sci. Instrum. **69**, 109–115 (1998).

[6]A. Degeling, H. Weisen, A. Zabolotsky, B. Duval, R. Pitts, M. Wischmeier, P. Lavanchy, P. Marmillod, and G. Pochon, "AXUV bolometer and Lyman-$\alpha$ camera systems on the TCV tokamak," Rev. Sci. Instrum. **75**, 4139–4141 (2004).

[7]L. Ingesson, J. Rapp, G. Matthews *et al.*, "Radiation in impurity-seeded discharges in the JET MkI, MkIIA and MkIIGB divertors," J. Nucl. Mater. **313**, 1173–1177 (2003).

[8]B. Peterson, G. Kawamura, P. L. van de Giessen, K. Mukai, H. Tanaka, R. Sano, S. N. Pandya, S. Y. Dai, S. Masuzaki, T. Akiyama, M. Kobayashi, M. Goto, G. Motojima, R. Sakamoto, N. Ohno, T. Morisaki, J. Miyazawa, and the LHD Experiment Group, "Experimental observations and modelling of radiation asymmetries during $N_2$ seeding in LHD," Nucl. Mater. Energy **26**, 100848 (2021).

[9]G. Kawamura, Y. Feng, M. Kobayashi, M. Shoji, T. Morisaki, S. Masuzaki, and Y. Tomita, "First EMC3-EIRENE simulations with divertor legs of LHD in realistic device geometry," Contrib. Plasma Phys. **54**, 437–441 (2014).

[10]S. Dai, M. Kobayashi, G. Kawamura, S. Morita, H. M. Zhang, T. Oishi, Y. Feng, D. Z. Wang, and Y. Suzuki, "EMC3-EIRENE modelling of edge impurity transport

in the stochastic layer of the large helical device compared with extreme ultraviolet emission measurements," Nucl. Fusion **56**, 066005 (2016).
[11]Y. Feng, H. Frerichs, M. Kobayashi, and D. Reiter, "Monte-Carlo fluid approaches to detached plasmas in non-axisymmetric divertor configurations," Plasma Phys. Controlled Fusion **59**, 034006 (2017).
[12]S. N. Pandya, B. J. Peterson, M. Kobayashi, K. Ida, K. Mukai, R. Sano, J. Miyazawa, H. Tanaka, S. Masuzaki, T. Akiyama *et al.*, "Dynamics of three-dimensional radiative structures during RMP assisted detached plasmas on the large helical device and its comparison with EMC3-EIRENE modeling," Nucl. Fusion **56**, 046002 (2016).
[13]T. Xie, S. Dai, G. Zuo, L. Wang, H. Zhang, B. Lyu, L. Zhang, J. Huang, J. Hu, Y. Feng *et al.*, "EMC3-EIRENE modelling of edge plasma and impurity emissions compared with the liquid lithium limiter experiment on EAST," Nucl. Fusion **58**, 106017 (2018).
[14]B. Peterson, S. Masuzaki, R. Sakamoto, K. Sato, S. Inagaki, A. Sagara, S. Ohdachi, Y. Nakamura, N. Noda, Y. Xu *et al.*, "The effect of divertor tile material on radiation profiles in LHD," J. Nucl. Mater. **290**, 930–934 (2001).
[15]O. Barana, A. Murari, P. Franz, L. Ingesson, and G. Manduchi, "Neural networks for real time determination of radiated power in jet," Rev. Sci. Instrum. **73**, 2038–2043 (2002).